Strål
säkerhets
myndigheten
Swedish Radiation Safety Authority

Authors: Philip Maul
Steven Benbow
Alex Bond
Peter Robinson

Research

2010:25

Modelling Coupled Processes in the Evolution of Repository Engineered Barrier Systems using QPAC-EBS

Report number: 2010:25 ISSN: 2000-0456
Available at www.stralsakerhetsmyndigheten.se

Title: Modelling Coupled Processes in the Evolution of Repository Engineered Barrier Systems using QPAC-EBS.
Report number: 2010:25
Author: : Philip Maul, Steven Benbow, Alex Bond and Peter Robinson.
Quintessa Limited, Henley-on-Thames, England.
Date: August 2010

SSM Perspective

Background

Currently in Sweden, the SR-Site safety assessment for a spent nuclear fuel repository is being developed by the Swedish Nuclear Fuel and Waste Management Company (SKB). The planned SSM review of this work requires access to a sufficient modelling capability to assess the combined performance of the engineered barriers (spent fuel canister, buffer and backfill) and the natural geosphere barrier. For the integrated safety assessment, capturing the interactions in between the both natural and engineered barriers is essential for evaluation of the containment phase and this usually requires a relatively large degree of simplification in the treatment of the individual barriers. Independent modelling capability can be used to check if key safety assessment results can be reproduced. Other types of implementation involve exploration of alternative conceptual models (ACMs), as well as parameters sensitivity evaluation and uncertainty analysis. A feasible approach for the handling of such issues is reported here (based on the QPAC-EBS modelling tool).

Purpose of the Project

The purpose of this project is to provide a brief summary of recent efforts to implement the QPAC-EBS code for evaluating different issues connected to the KBS-3 repository concept in Swedish granitic bedrock. This should give a rough idea of both the capabilities and the limitations of this code. Part of this work has been carried out within the now completed EU THERESA project.

Results

This report contains a range of modelling results from simplified performance evaluation of the KBS-3 repository concept. Example of important issues in which both the natural and engineered barriers are considered include the corrosion of copper canisters, possible erosion of buffer and backfill due to the infiltration of dilute glacial meltwaters, the resaturation of buffer, backfill and geosphere, and the thermal evolution of different components in the repository (mainly due to the residual heat from the spent fuel). It should be noted that results reported here are only illustrative and are only intended for evaluation of modelling capability.

Future work

The QPAC-EBS modelling capability and implementation can be extended and further developed based on future review priorities and new information from e.g. scientific experiments and site investigations. It has already been recognised that a more detailed model is required to review the combined buffer erosion – copper corrosion issue.

Project Information

Project manager: Bo Strömberg
Project reference: SSM 2010/1519
Project identification number: 3037023-05

Content

Executive summary

A satisfactory understanding of the evolution of repository engineered barrier systems (EBS) is an essential part of the safety case for the repository. This involves consideration of coupled Thermal (T), Hydro (H), Mechanical (M) and Chemical (C) processes.

Quintessa's general-purpose modelling code QPAC is capable of representing strongly coupled non-linear processes and has been used in a wide range of applications. This code is the basis for software used by Quintessa in studies of the evolution of the EBS in a deep repository for spent nuclear fuel undertaken for SKI and then SSM since 2007. The collection of software components employed has been referred to collectively as QPAC-EBS, consisting of the core QPAC code together with relevant modules for T, H, M and C processes. QPAC-EBS employs a fundamentally different approach from dedicated codes that model such processes (although few codes can represent each type of process), enabling the specification of new processes and the associated governing equations in code input. Studies undertaken to date have demonstrated that QPAC-EBS can be used effectively to investigate both the early evolution of the EBS and important scenarios for the later evolution of the system when buffer erosion and canister corrosion may occur.

A key issue for modelling EBS evolution is the satisfactory modelling of the behaviour of the bentonite buffer. Bentonite is a difficult material to model, partly because of the complex coupled mechanical, hydro and chemical processes involved in swelling during resaturation. Models employed to date have generally taken an empirical approach, but a new model developed during the EU THERESA project could be further developed to provide a better representation of these processes.

QPAC-EBS could play an important role in supporting SSM's review of the forthcoming SR-Site assessment by SKB if used by Quintessa in independent supporting calculations. To date radionuclide transport calculations following canister failure have been undertaken with separate software, but it would be possible, if required, to couple consideration of EBS evolution to radionuclide transport using QPAC's tracer transport module.

1. Introduction

A satisfactory understanding of the evolution of repository engineered barrier systems (EBS) is an essential part of the safety case for the repository. This involves consideration of coupled Thermal (T), Hydro (H), Mechanical (M) and Chemical (C) processes.

Quintessa's general-purpose modelling code QPAC [1] is capable of representing strongly coupled non-linear processes and has been used in a wide range of applications. This code is the basis for software used by Quintessa in studies of the evolution of the EBS in a deep repository for spent nuclear fuel undertaken for SKI and then SSM since 2007. The collection of software components employed has been referred to collectively as QPAC-EBS, consisting of the core QPAC code together with relevant modules for T, H, M and C processes. QPAC-EBS employs a fundamentally different approach from dedicated codes that model such processes (although few codes can represent each type of process), enabling the specification of new processes and the associated governing equations in code input. Studies undertaken to date have demonstrated that QPAC-EBS can be used effectively to investigate both the early evolution of the EBS and important scenarios for the later evolution of the system when buffer erosion and canister corrosion may occur.

QPAC uses compartments to discretise the system under consideration, as illustrated in Figure 1. Input is primarily file-based using block-structured text files, although applications for specific problems based on the code can be provided with a Graphical User Interface (GUI). The modelled system can be broken down into a number of subsystems with each subsystem being broken down into compartments (sometimes referred to as control volumes). Within each subsystem the same set of processes is considered in each compartment, but different processes can be considered in different subsystems. Cartesian or cylindrical polar grids of compartments/control volumes fixed in space can be used, but individually defined compartments (not in space-filling grids) need not necessarily have a fixed location in space.

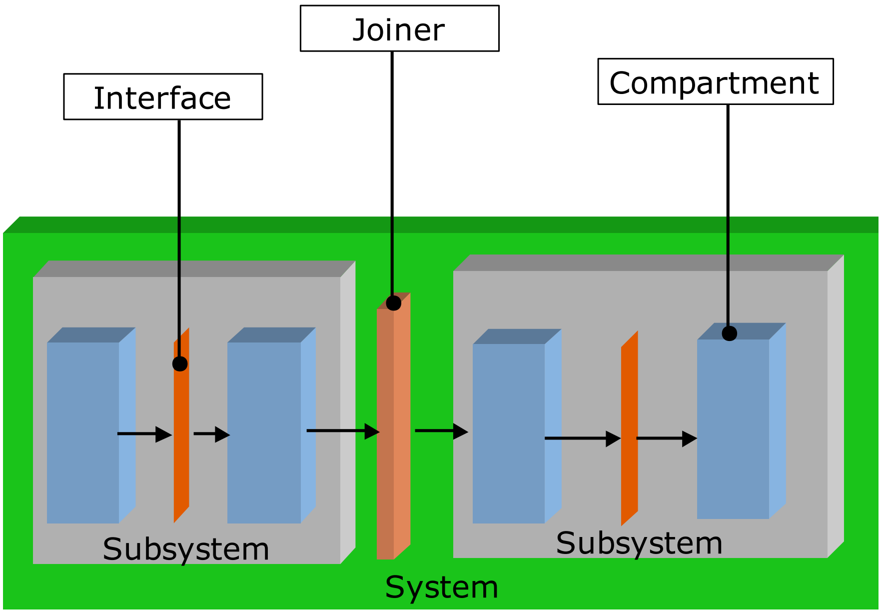

Figure 1
Discretisation in QPAC

The QPAC input syntax enables conceptual models for particular processes to be implemented. Alternatively, pre-defined models can be used that have previously been developed. QPAC can solve a general system of differential and algebraic equations within a compartmentalised system. The form of these equations is determined by the particular model being implemented. When a system of partial differential equations is to be solved, the discretisation of these equations is part of the model specification. Although QPAC does not impose the approach that is to be used for spatially discretising a system of partial differential equations, it is expected that the finite volume (or control volume) approach will be used. Advantages of this approach include:

- A structured grid is not required, although it can be used.
- Problems on irregular geometries can be considered.
- Because the flux entering a given volume is identical to that leaving the adjacent volume, all relevant quantities are readily conserved.
- Boundary conditions are easy to apply.

The alternative approach that is commonly used for continuum problems is the Finite Element approach. This shares some of the advantages of the finite volume approach, particularly in handling irregular geometries. The most significant difference between the approaches is in the way that fluxes between volumes are treated. In the finite volume approach there is a clear flux between volumes, ensuring that mass is conserved locally. In the finite element approach, there is no unique flux between elements – the normal gradients will generally differ across the interface – and local mass conservation is not always guaranteed. With the application areas that are envisaged for QPAC, local mass conservation and an ability to clearly see how mass is being transported through the system are important – hence the choice of the finite volume approach.

This report summarises the output of studies undertaken using QPAC-EBS. The information provided is taken mainly from Quintessa reports to SKI [2], [3] and reports and papers on Quintessa's contribution to the EU THERESA project [5], [6], [7]. The key results from the calculations that have been undertaken are described, but full mathematical details of the algorithms employed are not given here as these are provided in the referenced reports. The report is structured as follows:

- Section 2 describes QPAC-EBS calculations for thermal evolution;
- Section 3 considers repository resaturation;
- laboratory and full-scale test cases for the THERESA project are considered in Sections 4 and 5;
- modelling key processes in bentonite is considered in Section 6;
- chemical processes and buffer erosion are considered in Section 7; and, finally,
- the key conclusions to be drawn are given in Section 8.

2. Thermal evolution

Repository thermal evolution calculations using QPAC-EBS have been described in [2] and [3]. The models employed represent the governing equations for the transport of heat by conduction, convection and radiation. The analysis is undertaken for a single canister with a background heat source deriving from all the other canisters.

Although thermal processes are the most straightforward to represent, the separation of the canisters is critical for these calculations, and the SR-Can calculations [8] suggested that some canisters may come close to the imposed 100°C maximum temperature criterion.

The basis of the discretisation employed in the calculations is shown in Figure 2; the canister (assumed to be for BWR fuel) is surrounded by bentonite compartments and there is a backfill compartment at the top of the deposition hole. For simplicity the backfill characteristics were taken to be the same as those of the buffer. There can be gaps between the canister and the bentonite and between the buffer and the host rock; these are not shown explicitly in Figure 2 but are included in the model (and assumed not to change with time). The tunnel above the deposition hole was not represented explicitly (its properties were effectively assumed to be similar to the host rock) and there were several rock compartments surrounding the deposition hole. The Upper Buffer/Backfill and Lower Buffer regions shown in Figure 2 were split up into a number of compartments, using a cylindrical grid.

The outer boundary condition was determined by assuming that, at large distances from the source, the temperature drops off as the inverse square of the distance from the source. This was represented by assuming that the temperature falls linearly to ambient levels at a specified distance into a final heat sink compartment.

A simplified representation of the canister was employed as illustrated in Figure 3. Again, the air gaps between the different materials are not shown explicitly.

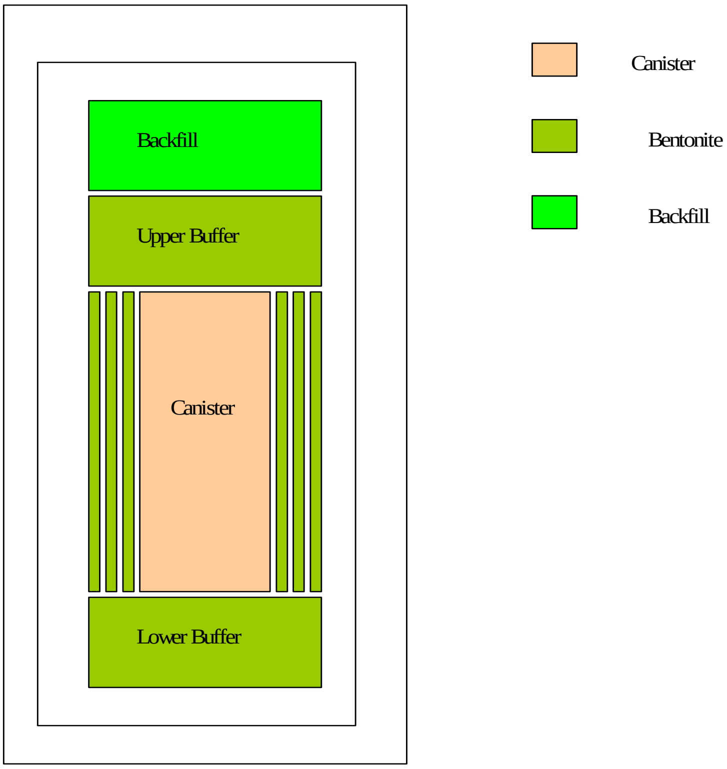

Figure 2
Regions in the thermal evolution calculations

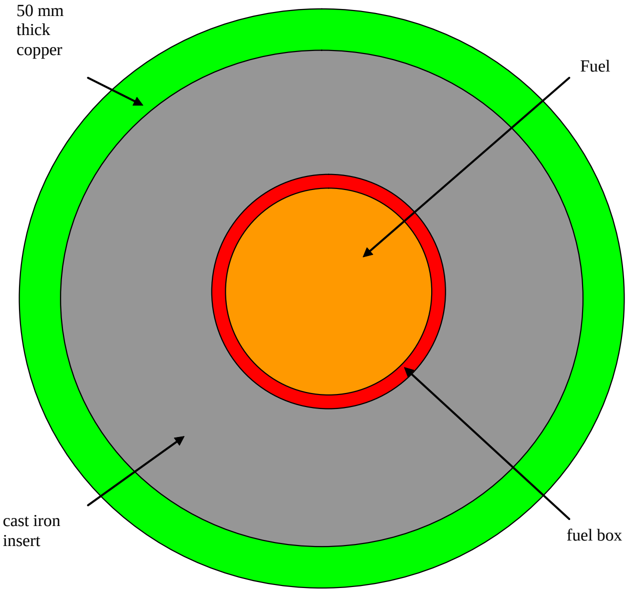

Figure 3
Simplified cylindrical geometry for the canister

Detailed analytical methods have been developed to represent the ‘background’ temperature rise due to neighbouring canisters [3]. There are uncertainties in the calculation of this background temperature because the way that the repository layout (the number of tunnels, their locations and separation, and the treatment of ‘rejected’ canister locations) was represented in SKB's thermal evolution calculations is not clear.

Using, wherever possible, the same parameter values as employed by SKB in the SR-Can assessment, the temperature at five locations was calculated: outside of the cast iron insert; outside of copper canister; inside of the buffer; outside of the buffer; and at the rock wall. These correspond to the outer five locations in Figure 9-17 of the SR Can main report [8]. In Figure 4 the QPAC-EBS calculations are compared with those presented in SR-Can. The SR-Can calculations are shown with thicker lines and larger symbols. The differences are up to about 3 degrees. A part of the differences seen here is due to the simple analytic model that SKB use for the canister (it has more geometric simplifications than the Quintessa model); SKB compared these to a fully 3D scheme and gets differences of the order of 1 degree [9]. The remainder of the discrepancy remains unexplained at the present time.

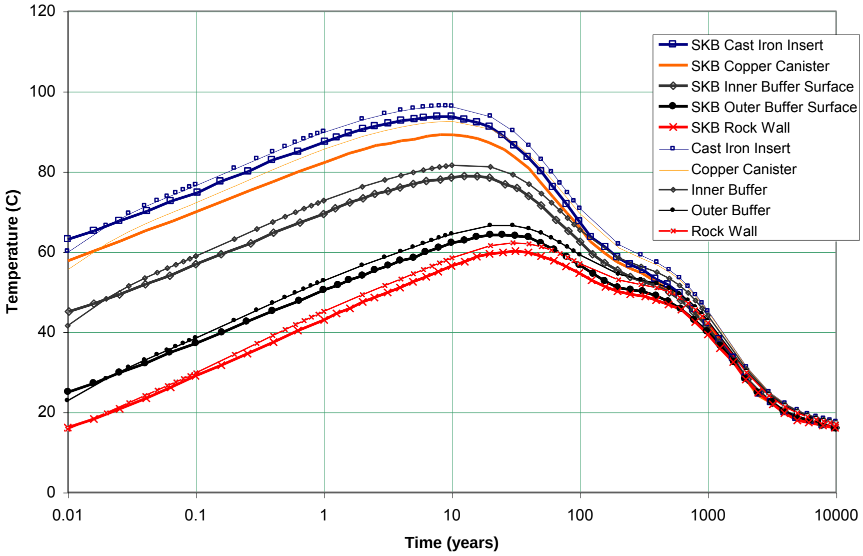

Figure 4
Comparisons between QPAC-EBS and SR-Can calculations

The sensitivity studies described in [3] showed that the key controls on peak temperature are the air gap between the can and buffer and the rock conductivity. Other changes in properties, the power function used for the source term and the number and locations of canisters only have small impacts on the peak temperatures. Without an air gap, peak temperatures would be 15 C lower. These calculations also showed that the resaturation timescale can be critical in determining peak temperatures.

3. Repository resaturation

Resaturation of the repository rock

QPAC-EBS calculations were described in [2] to study desaturation and resaturation of a deep repository. The model geometry was based on SKB's ConnectFlow calculations, consisting of a block of rock 8000 m by 6000 m by 1500 m deep [4]. As shown in Figure 5, the repository was represented as a single 'slab' 20 m thick at 400 m depth (Forsmark conditions) representing the disposal tunnels and associated host rock. The region was coarsely discretised with seven compartments in the X direction, five in the Y direction and five in the Z direction. The repository occupies the central compartment in all three axes. The calculations considered just the repository rock.

The external boundaries of the model were taken to be hydrostatic columns with atmospheric pressure at 0 m. Different conditions were applied at the top surface; it was effectively assumed that the model domain does not take an active part in the near-surface flow zone, and so zero recharge was assumed for all cases as initial conditions. Groundwater was assumed to have a constant density and viscosity. No gas dissolution was represented and air was assumed to behave as an ideal gas.

The reference calculation had the following features:

- Inflow to the repository was controlled by the backfill, with the permeability of the repository taken to be the same as the backfill.
- The groundwater was assumed to be unconfined, so that a pressure boundary condition at atmospheric pressure was applied with full gas saturation at the top surface (5m).
- Up to 25 mm y^{-1} extra recharge was available, applied as a pressure-dependent source of water in the UpperRock region. This represents additional recharge being available as the water is drawn down.

The final stages of the resaturation process can be very slow, and it is therefore difficult to define a unique time at which resaturation can be considered to be effectively complete. For the purposes of comparison with the SKB calculations, 'resaturation' was taken to correspond to the time when the repository compartment was 95% saturated. System equilibration times were taken to correspond to the time when pressures returned to 95% of pre-construction conditions.

Figure 6 and Figure 7 show the calculated evolution with time of the saturation and pressure in the repository for the reference case and for four variant cases with different assumptions about the surface boundary condition and rock anisotropy cases (details of which are given in [2]). The apparently linear evolution of water saturation is because the rate that water can be supplied is approximately constant.

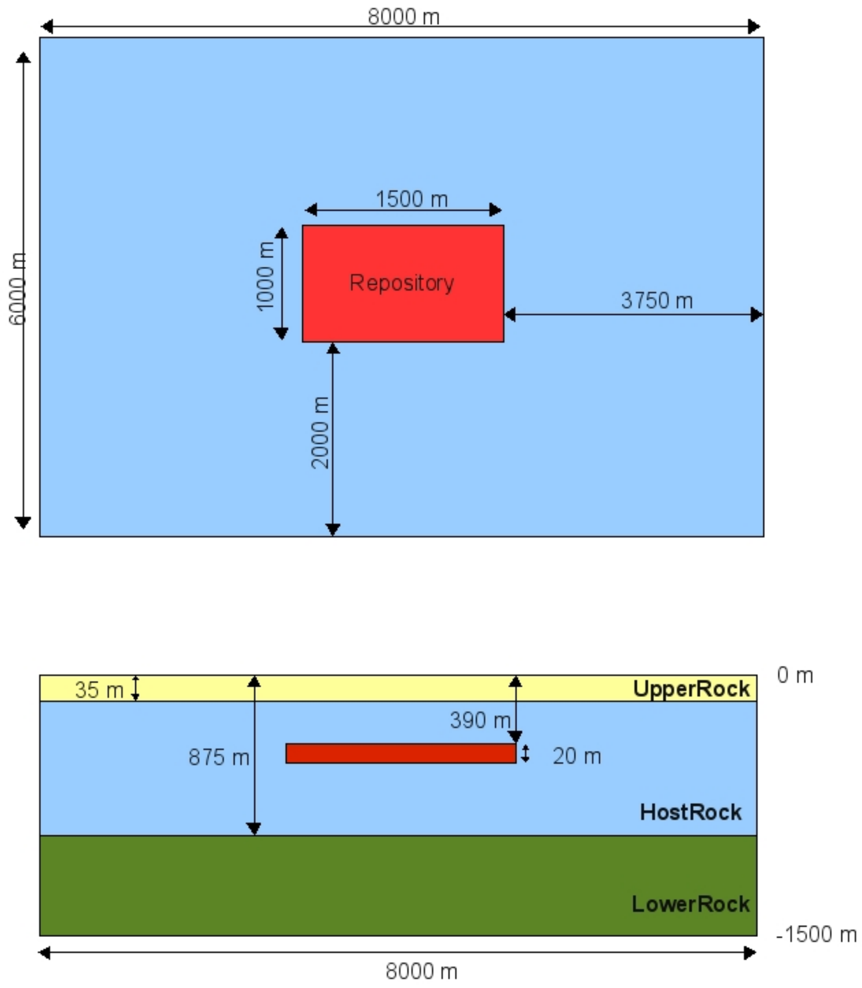

Figure 5
The modelled system for repository rock resaturation: plan (top) and section (bottom)

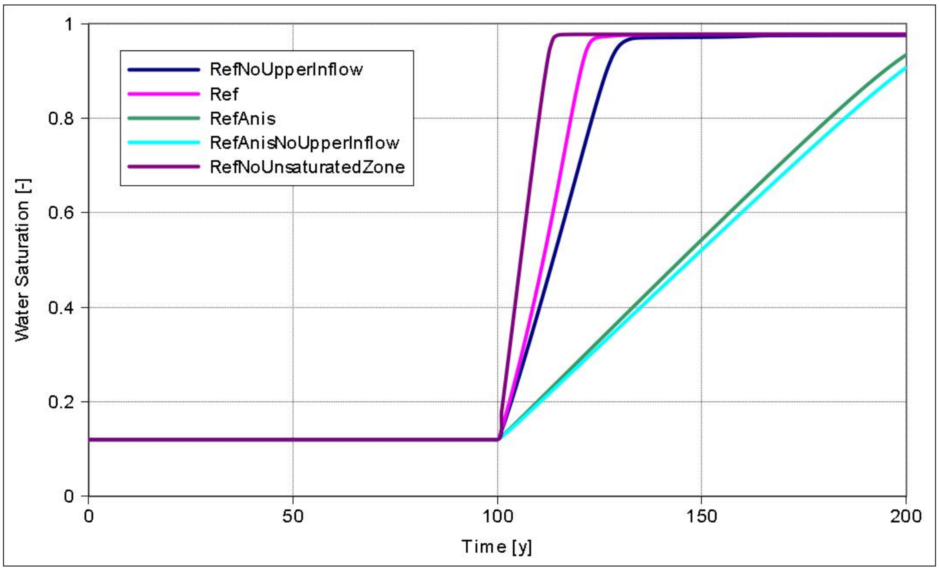

Figure 6
Repository resaturation calculations

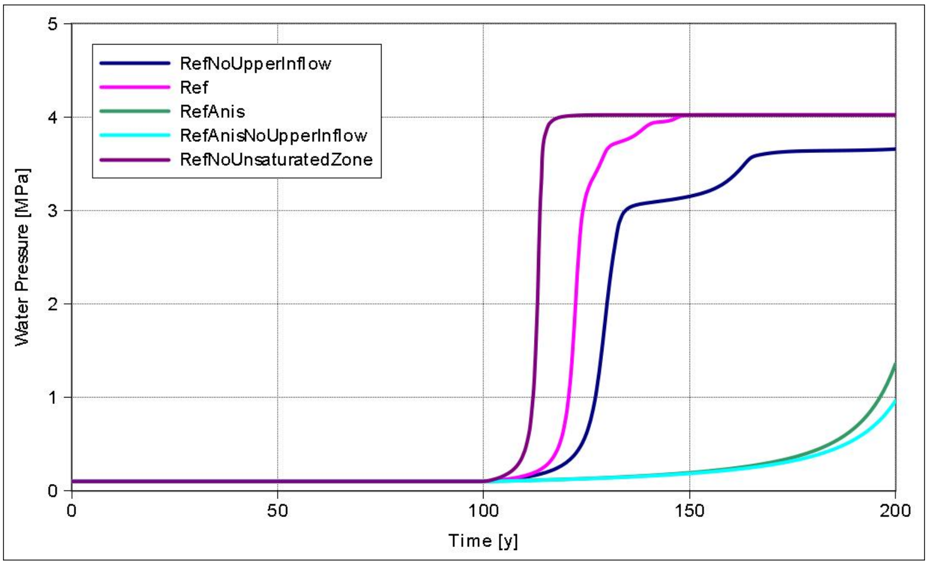

Figure 7
Repository pressure evolution calculations

The resaturation timescales obtained in the QPAC-EBS calculations were generally consistent with the relatively short timescales calculated by SKB. However, timescales of much greater than 200 years can be obtained with some combinations of modelling assumptions. As would be expected, the hydraulic conductivity of the host rock and backfill are dominant. This illustrates the wide range of resaturation times that could be seen and emphasises that further consideration needs to be given to this question. The representation of the unsaturated zone and the choice of relative permeability curves would need further consideration in future calculations using QPAC-EBS.

Bentonite resaturation

In [3] the resaturation of the bentonite buffer was modelled using the original model for bentonite employed in the THERESA Project [6]. A single deposition hole was modelled with the bentonite above the canister being represented explicitly but the rock and tunnel backfill were replaced by boundary conditions. The modelled system extended radially to half the designed canister separation distance. The canister itself was represented as a single compartment in a separate subsystem where only the thermal processes were considered.

The system grid used in the QPAC-EBS calculations is shown in Figure 8. It should be noted that the key variables such as pressure and temperature are calculated on the interfaces between compartments as well as in the compartments: this almost doubles the effective resolution achieved.

Two sets of coupled calculations were considered, with the first representing high geosphere water availability and the second low geosphere water availability:

- Resaturation from a ‘wet’ host rock (95% water saturated) with all outer boundaries at hydrostatic water pressure. Initial air pressures in the host rock are hydrostatic. Inflow to the buffer is expected to be very high.

- Resaturation from a drier host rock (75% water saturated) with no-flow for water and air on the radial and lower boundaries, and only air exchange (at atmospheric pressure) across the top boundary. Initial air pressures in the host rock are atmospheric. Water inflow to the buffer is expected to be very low.

In each case the bentonite was initially at a water saturation of 67% and initial air pressure of atmospheric. These two cases are expected to bound likely resaturation behaviour and hence represent extreme examples.

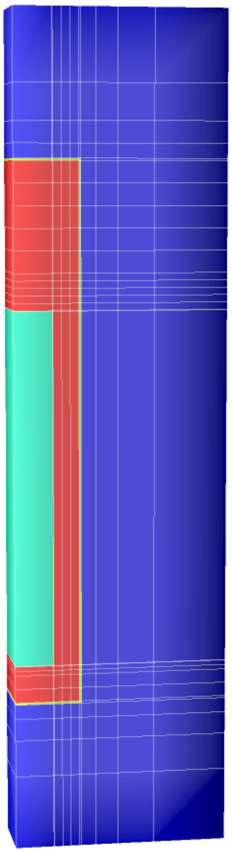

Figure 8
Radial model domain showing the system grid employed in QPAC-EBS for bentonite resaturation calculations

For the thermal processes the outer boundaries were specified using a prescribed thermal flux, obtained by calculating the difference in the temperature at the boundary and the 'background' temperature. Capillary curves for bentonite were selected from the detailed analysis available for buffer behaviour [6]. For the host rock, development of a single representative capillary curve is extremely difficult and a simplifying assumption was adopted by using the bentonite capillary curve, but with a factor of ten reduction in capillary pressure for a given saturation, based on expert judgement in the absence of definitive data [24].

The processes modelled are:

- viscous flow of gaseous air;
- viscous flow of liquid water;
- dissolution and transport of air in water;
- water vapour generation and migration through diffusion and advection of air;
- thermal conduction;
- advective heat migration (air, liquid water and water vapour);
- radiation (not used in these calculations);
- latent heat of vaporisation and condensation; and
- porosity-dependent permeability for bentonite.

The water saturation calculations for the ‘dry’ host rock are shown in Figure 9. The impact of the high suction of bentonite, and the low porosity of the host rock, results in the relatively slow transport of the porewater from the host rock and reduction of the degree of saturation from the starting value of 0.75 to almost zero. Canister heating results in the production of water vapour in the bentonite, but this effect is dominated by the ability of the bentonite to draw water in from the host rock when it is in hydraulic contact. The initial gaps (not represented in this calculation) between the bentonite buffer and the host rock initially will limit this hydraulic contact until sufficient water has filled the gap to cause the bentonite to swell up to the rock interface.

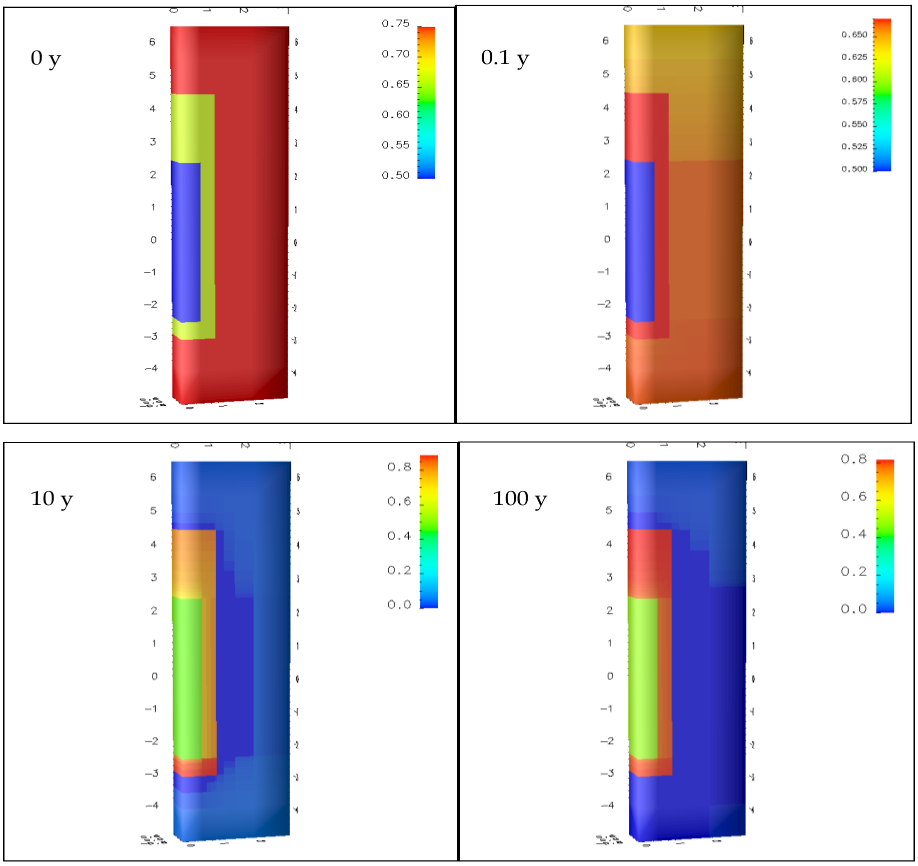

Figure 9
Calculated water saturations for the ‘dry’ case. Different scales are used on each picture and the canister saturation is fixed at 0.5 so it can always be identified clearly. Colours show compartment-averaged values.

For the ‘wet’ case (Figure 10) resaturation occurs rapidly due to the relatively high water pressures in the host rock and the high suctions in the bentonite which draws in water rapidly, with the sides and lower portion of the bentonite largely resaturated after only two years. The upper portion of the buffer takes until just beyond five years to resaturate. Hydraulic equilibrium is achieved after approximately 15-20 years. Again, a gap between the buffer and rock may increase resaturation times as hydraulic continuity between the buffer and host rock will not be established until the bentonite swells. Evidence from the Canister Retrieval Test (see Section 5) and other sources indicates that this will occur rapidly after significant amounts of water are present in the gap.

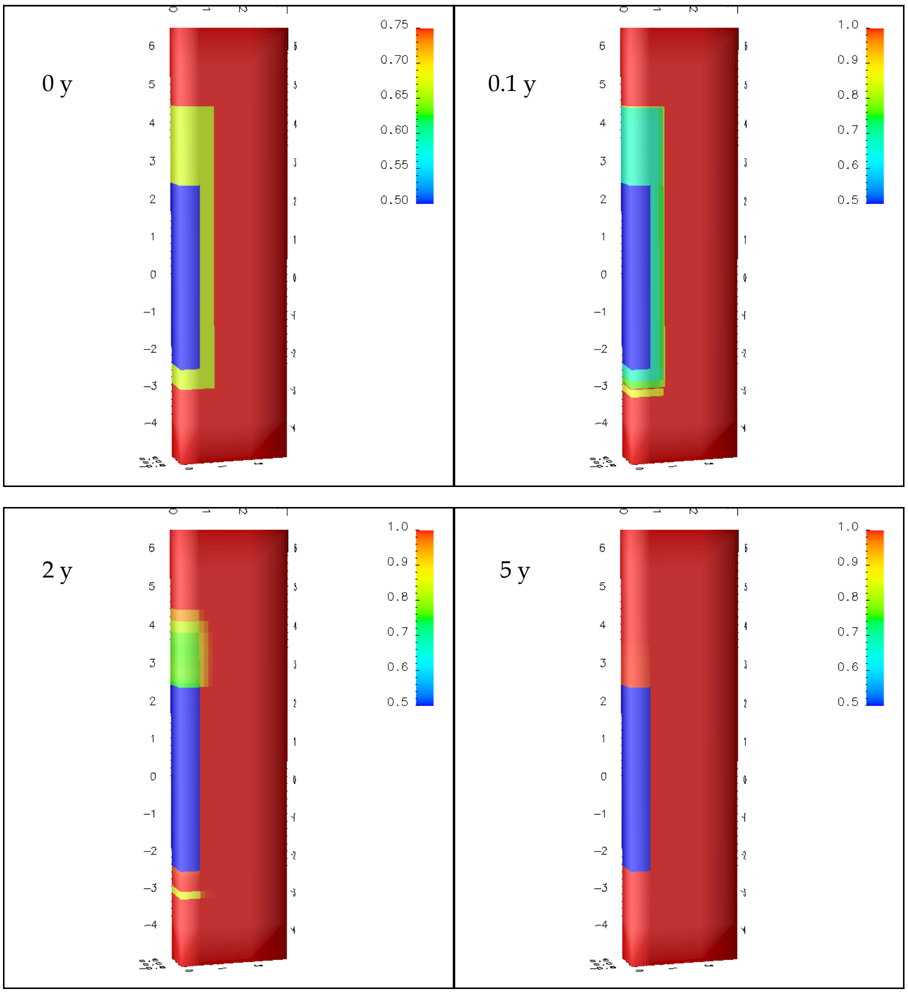

Figure 10
Model water saturations for the ‘wet’ case.

4. Bentonite resaturation: the THERESA test cases

Introduction

The THERESA project (short name for “Coupled thermal-hydrological-mechanical-chemical (THMC) processes for application in repository safety assessment”) was an international co-operative research project sponsored by the European Commission under its FP6 programme. The overall objective of THERESA was the development of a scientific methodology for evaluating the capabilities of mathematical models and computer codes used for the design, construction, operation, performance assessment, safety assessment, and post-closure monitoring of geological nuclear waste repositories. The project took place over a three-year period from the start of 2007 to the end of 2009. Quintessa participated in this project with support from SKI and then SSM.

The use of QPAC-EBS for the THERESA benchmarking test studies is described in [5]. All three test cases involved the calculation of relatively small (cm to m scale) bentonite evolution under resaturation conditions. Each examined different configurations of available external water (Case 3 having no external inflow of water), mechanical confinement, applied heat and different bentonite properties.

A number of model quantities had to be calibrated to the available laboratory data. The key aspects of the model that was used to represent important processes in bentonite are discussed in Section 6.

Thermal evolution

Due to the configuration of the laboratory experiments and relatively well understood properties and processes associated with heat transfer, the thermal evolution of the system was straightforward to conceptualise and model. The most complex case to match well was the thermal gradient variant of Case 2 where the latent heat of vaporisation was critical to achieving the correct transient thermal evolution, which in turn constrained the hydraulic evolution; in this case it was essential to represent the coupling between processes correctly and this was achieved using QPAC-EBS. In all other cases the hydraulic-thermal coupling was insignificant.

Hydraulic evolution

The understanding of hydraulic evolution was largely through measured relative humidity (Case 1 and 2), the total amount of water entering the system (Case 1 and 2) and the measured water content at the end of the experiment (Case 1 and 3). In all a good qualitative and quantitative match to the observed data was obtained using a broadly consistent set of parameters and hydraulic models for relative humidity and water content. Illustrative results are shown Figure 11.

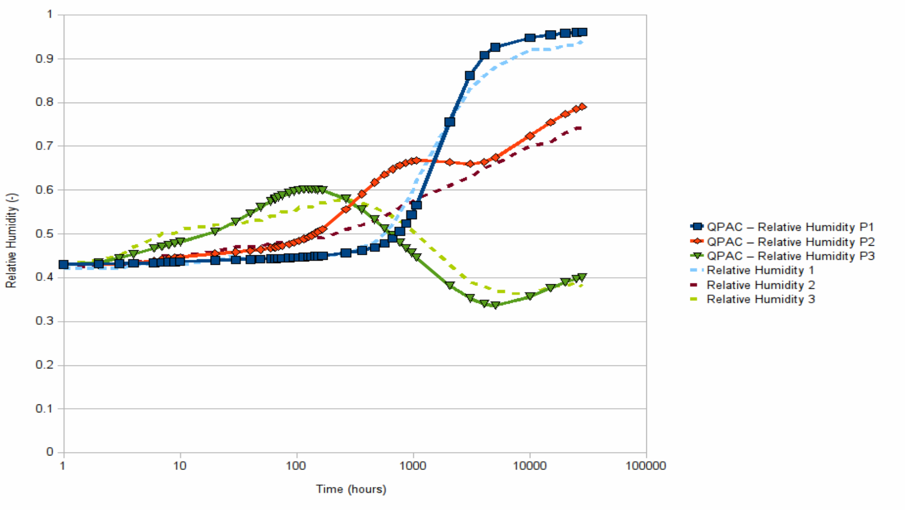

Figure 11
Relative humidity for Case 2 with applied thermal gradient

Difficulties in obtaining good fits with the experimental data were limited to understanding the total amounts of water measured entering the samples during the resaturation process. Both Cases 1 and 2 gave estimates of water ingress that would have saturated the samples 2-3 times over. Similar problems were experienced with other codes that participated in the benchmarking exercise, indicating that experimental problems may have been experienced through leakage.

Mechanical evolution

Cases 1 and 3 gave the opportunity to understand the mechanical evolution in terms of stresses (when confined – Case 1) and swell displacements (when largely unconfined – Case 3). As can be seen in Figure 12 (Case 1), the qualitative aspects of the system behaviour were well represented; one would expect this given that inputs to the model included the fully confined swelling pressure, based on experimental data. However, it proved difficult to explain some of the details of the observed behaviour. For Case 1 the details of the transient behaviour are hard to match without developing an overly complex model of swelling pressure with changing saturation. For Case 3, the general behaviour was again represented well, but the details, in particular the point at which zero radial swelling occurs, is difficult to reproduce with the simple mechanical and swelling models employed.

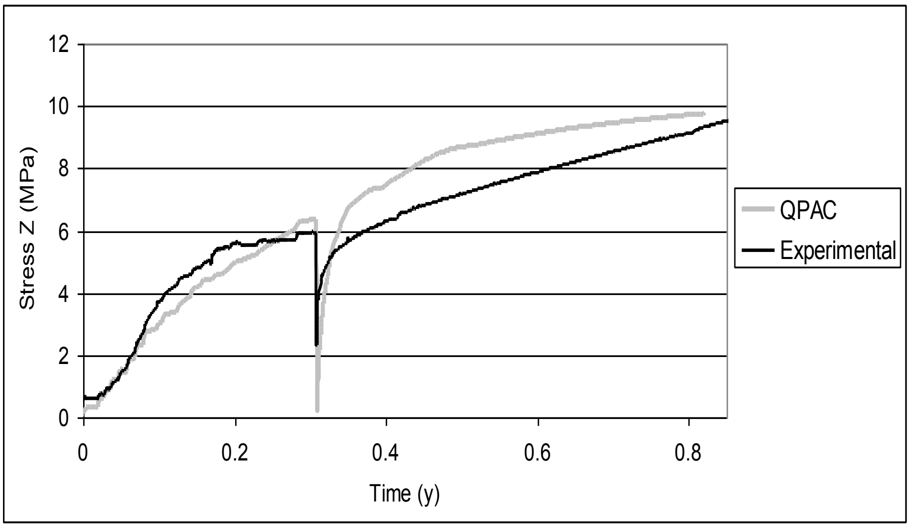

Figure 12
Vertical stresses, Case 1 (cell 1 for phases 1 and 2)

Summary

The THERESA test cases showed that in general the THM behaviour of a water-bentonite system can be reproduced well using QPAC-EBS. Some of the details of the system evolution, particularly with regard to swelling and mechanical deformation, are more difficult to reproduce. The adequacy of this representation depends on the application, and specifically the needs of the relevant safety case.

5. Bentonite resaturation: the CRT experiment

SKB’s Canister Retrieval Test (CRT) involved the resaturation of the bentonite around a full-scale disposal canister, with the gap between bentonite blocks/rings and the rock wall being filled with bentonite pellets. The test is shown schematically in Figure 13. This was used as the basis for the full-scale test case in the THERESA project.

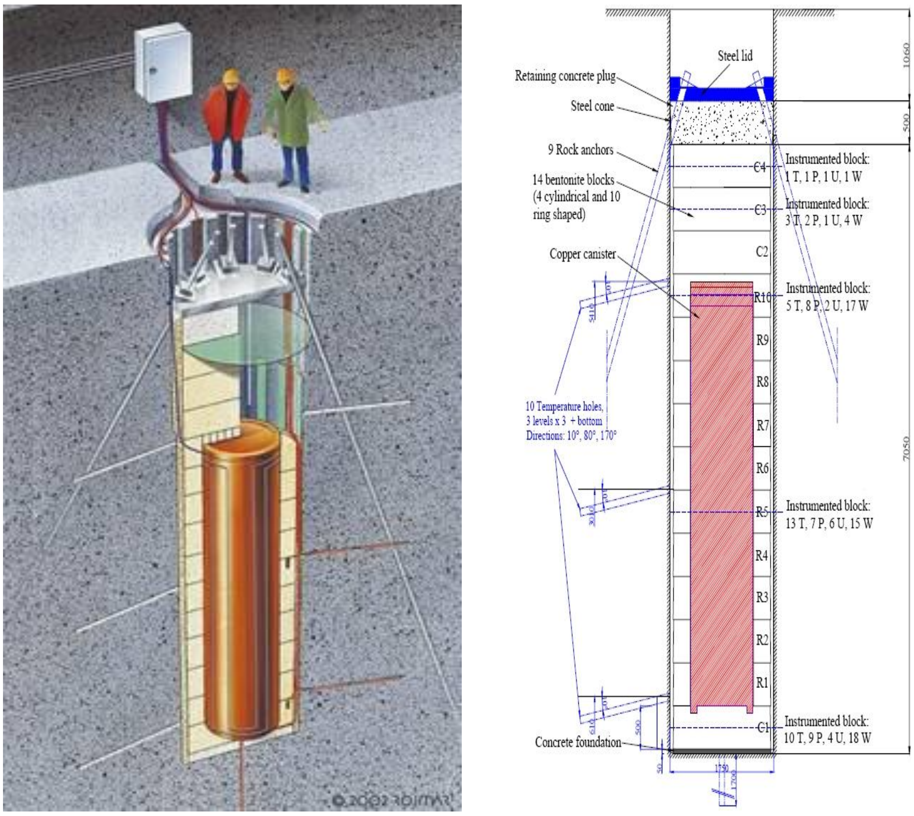

Figure 13
The Canister Retrieval Test

Ring-shaped or cylindrical bentonite blocks were placed in the hole. At the top of the canister bentonite bricks filled the volume between the canister top surface and the top surface of the upper most ring. The volume between the bentonite blocks and the hole wall was filled with bentonite pellets and water. On top of the plug a steel lid was installed. The plug and lid could move vertically and were attached to the rock by nine rock anchors.

The test was installed in autumn 2000. The canister, equipped with electrical heaters, was lowered down in the centre of the hole. Additional bentonite blocks were emplaced until the hole was filled to a distance of one metre from the tunnel floor. The top of the hole was sealed with the retaining plug, secured against heave caused by the swelling clay with the nine cables anchored in the rock. Water was supplied artificially for saturation around the bentonite blocks.

As part of the THERESA project both 1D and 3D calculations were undertaken and compared with experimental data; some examples from the 3D calculations are given here. The 3D model domain, constructed as a cylindrical geometry with the axis of radial symmetry running centrally through the centre of the canister, is illustrated in Figure 14.

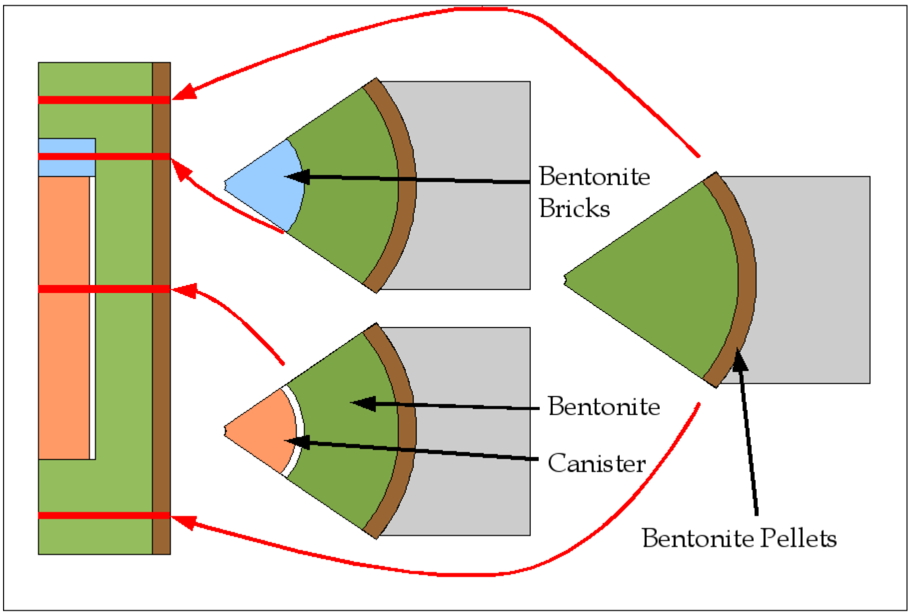

Figure 14
System geometry for the 3D CRT calculations

The calculations involve the modelling of complex coupled THM processes, as illustrated in Figure 15.

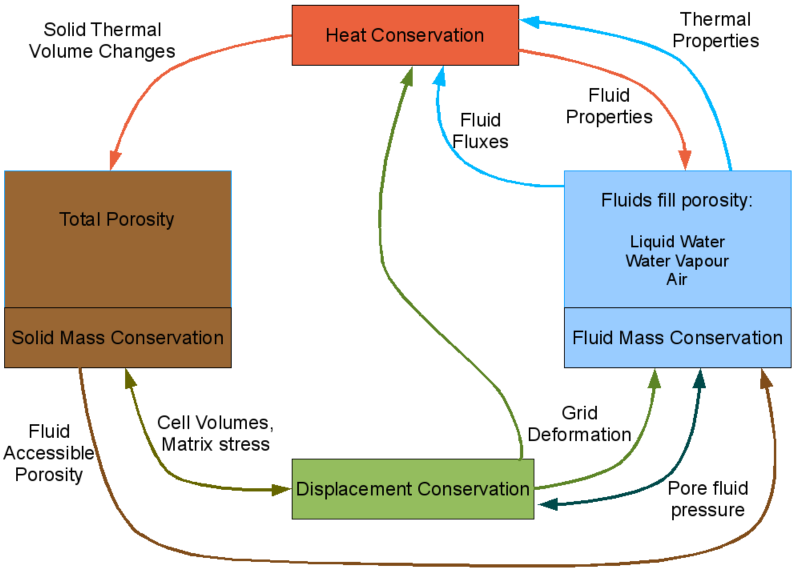

Figure 15
Process interaction diagram

Comparisons between calculations and measurements for the thermal and hydraulic evolution of the system were good, consistent with the results for the benchmark test cases, but the QPAC-EBS calculations tended to over-predict the amount of water that entered into the centre of the bentonite.

The calculations of cumulative water ingress (Figure 16) over-predicted the amount of water entering the system by the end of the experiment by approximately 15% and do not completely reproduce the ‘steps’ seen in the measurements. The overall impression is that, if the water ingress data are believed to be reliable, the bentonite system ‘seals’ against a given applied input water pressure. In order to get more water into the bentonite one then has to apply an excess pressure. If this ‘sealing’ process is real, this could be important for repository resaturation timescales.

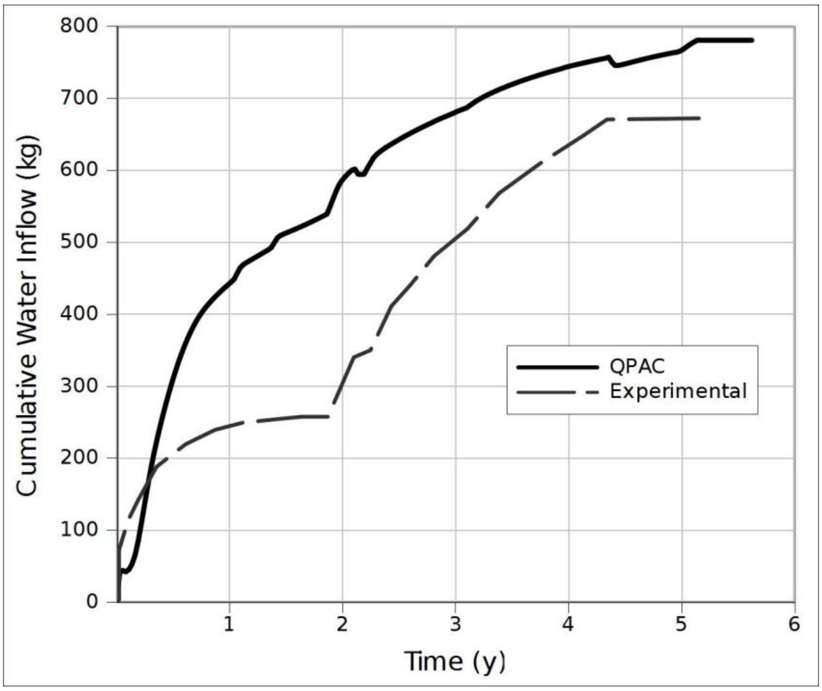

Figure 16
Calculated and observed cumulative inflow of water to the bentonite buffer

Figure 17 shows the measured and calculated plug displacement. The boundary condition applied ensures that the total force applied is consistent with the measured net displacement, with a 20 mm displacement being approximately equivalent to 8000 kN. The comparison is good, but the QPAC-EBS calculations tend to show a more rapid increase in vertical stresses during the middle period of the experiment and slightly higher stresses at the end of the simulation. Both of these observations are consistent with the apparent over-estimation of water ingress into the system; the representation of mechanical swelling and deformation appears to be appropriate.

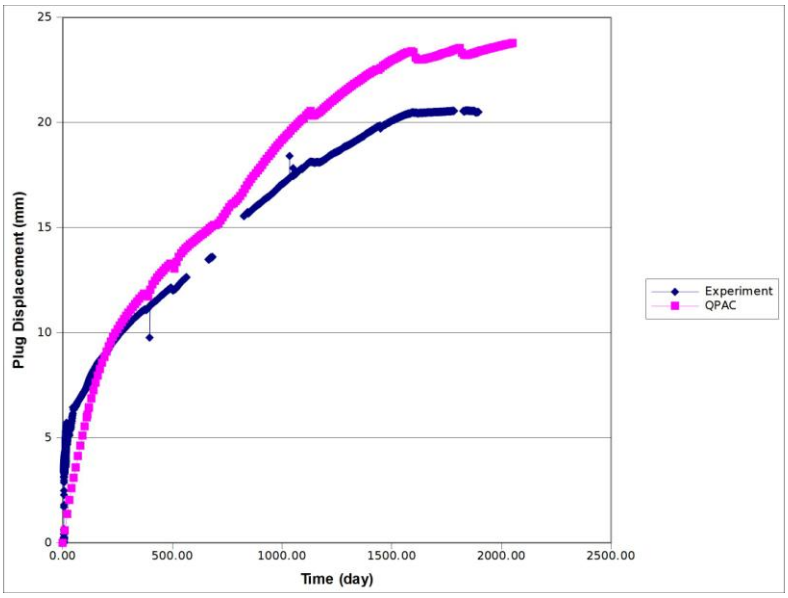

Figure 17
Calculated and measured plug displacement

The calculated and measured final dry density for Ring 10 is shown in Figure 18. The final dry densities match extremely well for the pellets and ring bentonite, but small deviations are seen in the brick and cylinder bentonite regions. Consistent with the observations on hydraulic evolution, there appear to be some differences in the mechanical behaviour of the rings and cylinders. There appear to be significant property variations between bentonites that have been processed and manufactured using slightly different techniques.

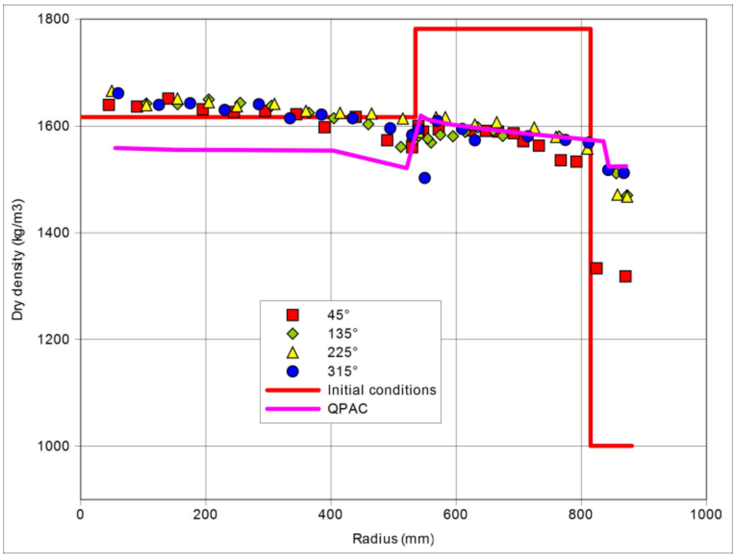

Figure 18
Comparisons between calculated and measured dry density at the end of the experiment for Ring 10

The over-prediction of the rate of saturation could possibly reflect the limitations of an elastic-only mechanical model (as used in these calculations). However, if the suction pressure is the cause of the problem, then it implies that the implementation of the conventional approach to capillary curves could be improved when dealing with bentonite, especially for partially-confined bentonite. This coupling of the macro-scale suction curve to the hydro-mechanical properties of bentonite is one of the key features of the more detailed model for bentonite discussed in Section 6.

There appears to be scope to investigate the possible variation of hydraulic and mechanical properties between different blocks of bentonite. However it must be emphasised that overall the comparisons between the QPAC-EBS calculations and the experimental measurements were excellent considering the complexity of the system and the processes involved.

6. Modelling key processes in bentonite

Introduction

Most THMC models use algorithms for the hydro and mechanical properties of materials that derive from data obtained from soils and rocks. Relevant hydro processes include the representation liquid and vapour transport using the concept of intrinsic and relative permeabilities, and the calculation of capillary pressures as functions of pore saturation. This general approach has also been applied to bentonite, despite the fact that in many ways bentonite properties are very different from those of soils and rocks. This problem has been recognised by several workers in the field, and there have been attempts to understand the properties of resaturating bentonite using a more self-consistent approach (e.g. [10]).

The model employed in the THERESA calculations described in Sections 4 and Section 5 is here referred to as the ‘old’ model. A ‘new’ model has been developed that aims to represent the disposition of water in the material in a more realistic way. It is considered that this model should be a better starting point for representing key hydro and mechanical processes, and may also be appropriate to use when chemical processes need to be considered. Fuller details are given in [6].

The old model

In this model a distinction was made between ‘free’ and ‘bound’ water in bentonite. The ‘free’ water was assumed to be available for flow, but the ‘bound’ water was assumed to be immobile.

A number of parameters require calibration against laboratory data. Quantities concerned with hydro processes include: the bentonite intrinsic permeability; the air entry pressure; the vapour diffusivity; the suction pressure at zero saturation; and the fraction of water in the bound state. Quantities concerned with mechanical processes include: the swelling pressure; the swell strain response; the vertical/radial swell strain bias; and Young’s modulus for bentonite.

The new model

Water can be considered to be present in bentonite in four forms as shown in Figure 18:

- Interlayer water: liquid water held between the clay interlayer sites, sometimes referred to as ‘crystalline’ water. This water is assumed to be immobile (in the sense that it is not available for flow).

- Double-layer water: liquid water held in the double layer around the perimeters of grains. This water is also assumed to be immobile.
- ‘Free’ water: water held in liquid form in the free porosity. This water is mobile and would be recognised as the water phase is standard unsaturated flow theory.
- Water vapour: water held as vapour in air in the free porosity. Water in this state will advect with air and can diffuse in the air rapidly.

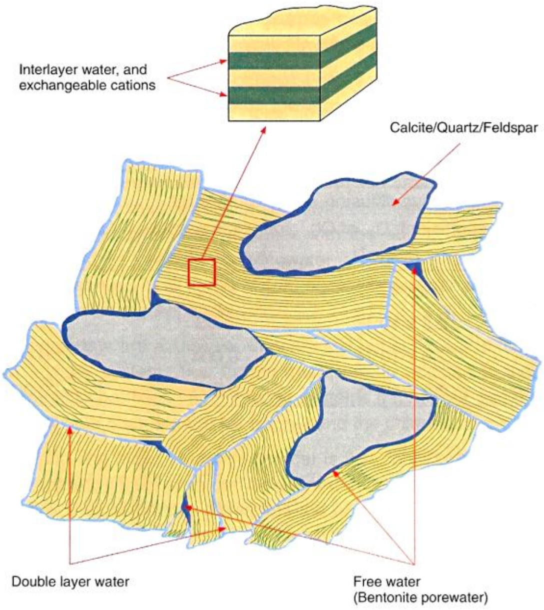

Figure 19
Water in bentonite: schematic from [11]

At low saturations, the fraction of water held in interlayer water is very high (represented by high suctions in simple capillary pressure models) and negligible amounts of water exist in all other liquid forms. As water saturation increases, the amount of water in the other forms rises, such that only at high saturations is there a significant amount of liquid water in the free porosity. Movement of liquid water therefore only occurs at the highest saturation levels, otherwise internal movement of water is probably dominated by the local migration of water vapour.

Swelling of compacted bentonite is thought to be primarily caused by the effect of water filling the interlayer sites and effectively increasing grain volume, although some limited swelling may occur from the saturation of the double-layers.

The use of ‘porosity’ and ‘saturation’ as key properties (as is typically used in other porous media) as applied to total water is potentially misleading when considering bentonite. In this model amounts of water in different states are considered. Only the free water, water vapour and air are relevant to conventional multiphase flow modelling; the rest of the water is effectively treated as part of the solid phase.

Consistent with the discussion of the conceptual model, the following definitions are employed:

- Free porosity: the fraction of a given volume not filled by solid materials and implicitly assumed to be available for saturation by liquid water, water vapour or air.
- Free liquid water saturation: the volumetric fraction of the free porosity that has been filled by liquid water.
- Water vapour saturation: the volumetric fraction of the free porosity that has been filled by water vapour.
- These are the porosities and saturations that would be usable in standard models of multiphase flow.

The multi-phase flow (MPF) model used in QPAC-EBS includes a model for the partitioning between water vapour and liquid water. This model uses the total suction pressure and temperature to define a relative humidity, which in turn can be used to calculate an effective saturation of water vapour in the open porosity volume.

A kinetic approach to water partitioning can be employed which requires no further parameterisation. Thermodynamic energy minimisation is considered, whereby water will always move from the higher pressure (equivalent to energy density) state to the lower pressure state. Thus while the free energy of interlayer water is less than that of vapour (for example), water will move from the vapour state to the interlayer sites.

This approach has the benefit of being able to use the free energy and water pressure directly to determine the disposition of water, with only the specification of appropriate kinetic rates. The rates are defined so that they are sufficiently fast that such transfers do not significantly affect the overall behaviour of the system, but not so fast that the timestepping used by the QPAC solver is significantly affected. These rates are therefore not currently constrained directly by physical considerations, but such considerations could be taken into account if relevant data became available.

The portion of the free energy assumed to be associated with liquid (free) water was calculated by estimating the point at which significant free water became present in the experiments reported in [12]. This was taken to be when the water content was equivalent to an average of 3.5 interlayers of water uptake by the bentonite grains. Thus the bulk free energy curve can be separated into two parts, as shown in Figure 20: the first relating to the interlayer water, and the second for all remaining forms of water (assumed to be ‘free’).

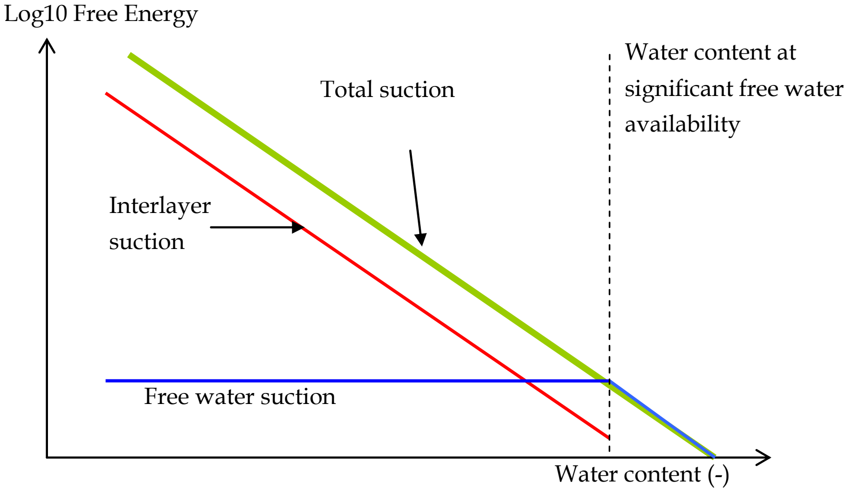

Figure 20
Schematic illustration of the breakdown of the suction curves given in [12]

In order to calculate the suction curves one simply multiplies the free energy by the molar density of bentonite. This approach gives a direct means to relate the amount and saturation state of the bentonite to the observed suctions in the system.

The mechanical model used in QPAC-EBS 'creates' additional strain in the system in response to the swelling caused by water filling the interlayer and double-layer sites through a simple interpolation between zero swell stress (initial conditions) to a maximum swell stress (fully saturated), where the saturated swell stress is derived from experimental results. Adding interlayer and double-layer water causes the effective volume of the bentonite grains to change and hence causes stresses to be induced in the grain structure and the free porosity to be reduced. The amount of bulk strain induced by swelling is calculated directly from the effective volumetric change in grain sizes at the microscopic scale.

Example calculations with the new model

The observed suction curves for bentonite under confined and unconfined conditions can be calculated as an output of the model. Equally, the calculated swell stress under variably confined conditions, assuming a suitable mechanical model, is also as a model output that can be compared with experimental data.

Simplified calculations have been undertaken to test whether the basic conceptual model is sound. Only one type of immobile water, interlayer water, was considered, assuming that this is solely responsible for the bentonite swelling behaviour. A range of representative experimental data was collected to give the following input data sets:

1. Unswelled and swelled bentonite molar volumes in order to understand the water ‘capacity’ of swelled bentonite.
2. Potential energy studies of pure bentonite, most notably[12]. This allowed the potential energy of interlayer water versus ‘free’ water to be evaluated in unconfined conditions at different water contents.
3. Chemical make-up and variability of MX-80 bentonite in order to be able to include the above two data sets in a full model. From this it was calculated that an MX-80 bentonite was approximately 75-80% ‘pure’ bentonite as measured in [12].
4. A simplified mechanical model that increases the stiffness of the bentonite asymptotically as the free porosity is reduced to zero, i.e. the bentonite block starts to behave as a single ‘grain’ and less of a compressible porous medium.

Using the default parameterisation for the CRT cases, a series of tests was conducted to see if the new model could reproduce observed macro-scale swelling tests in terms of confined swelling pressure at different dry densities and also reproduce bulk suctions measured in variably saturated bentonites. Illustrative calculations are shown in Figures 21 and 2. These calculations show that the model reproduces the observed swelling pressures well for the CRT cases, while the confined suction pressures, albeit a little on the low side, are also a reasonable match. Under these tests one observes that the interlayer water is approximately 65% ‘saturated’ (approximately equivalent to two interlayers of water) and the free porosity has decreased to approximately 11%. Both of these observations are consistent with various analyses available in the literature and noted in [6].

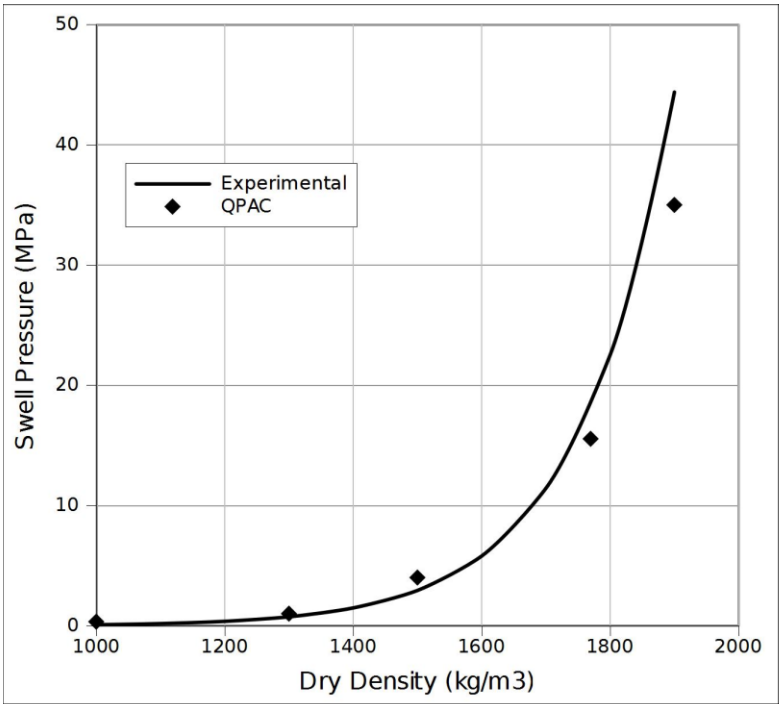

Figure 21
Comparisons between experimental data and calculations for the fully confined swell stress using the new bentonite model

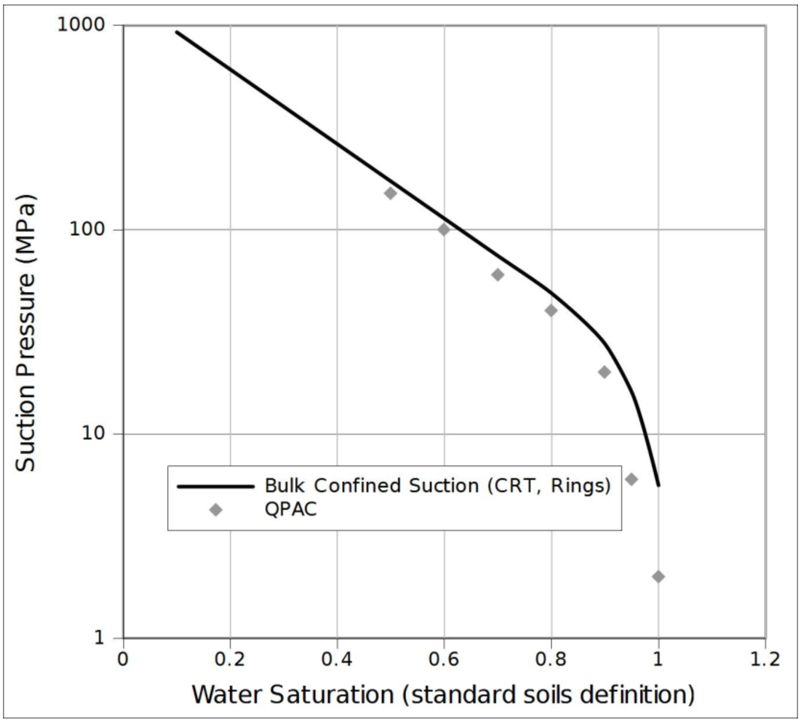

Figure 22
Comparisons between experimental data for bulk fluid suctions in the CRT ring sections and calculations using the new bentonite model

7. Chemical processes: buffer erosion and canister corrosion

Introduction

SKB consider that erosion of the buffer is a potentially important factor in the performance assessment of a deep repository for spent fuel [8]. Erosion is caused by the interaction of dilute glacial meltwaters with the buffer, which can act to destabilise and remove some of the buffer material. For extreme amounts of loss of buffer material by erosion, the buffer swelling pressure can potentially fall below the critical value required by the relevant safety function, so that this safety function could not be sustained in the following period.

In order to investigate the effect of buffer erosion on canister corrosion it is necessary to consider both the physical and chemical evolution of the buffer and couple this to the transport of corrodants. Some calculations were undertaken in 2008 using QPAC-EBS to demonstrate this coupling [3]. These calculations test various aspects of the QPAC-EBS code and check if processes relevant for the KBS-3 concept can be incorporated. The modelling assumptions and parameter values are very preliminary and would have to be evaluated and revised before model calculations could be used in safety evaluation.

The calculations assumed the geometry shown in Figure 23, which is the same geometry considered by SKB when modelling the physical erosion processes in [13]. The purple area in Figure 23 indicates the region where bentonite may enter fractures as a gel following expansion of the bentonite aggregates during repository resaturation. Erosion is assumed to take place at the tip of this intrusion when the bentonite gel comes in contact with dilute waters. For the chemical alteration, a similar set of processes to those assumed by SKB in [14] were considered. Models of increasing complexity were developed, with processes being added gradually, so that the importance of the different processes can be assessed before fully coupled QPAC-EBS calculations can be undertaken.

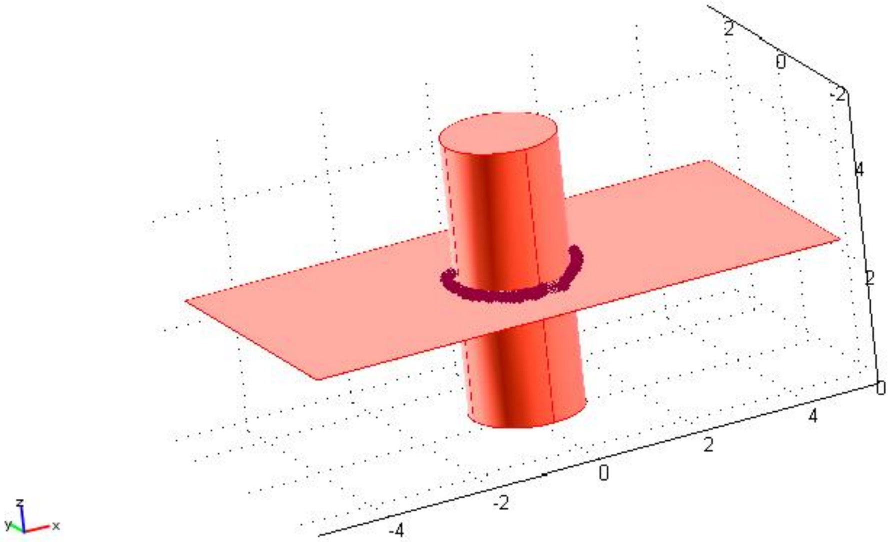

Figure 23
System geometry assumed in [13]. The planar feature represents a fracture intersecting the cylindrical deposition hole.

Chemical modelling

SKB have modelled the chemical evolution of the buffer in [14]. The SKB model of MX-80 bentonite includes processes for

- solubility of trace minerals (gypsum and quartz);
- ion exchange between Na-Ca-Mg-K montmorillonite;
- surface complexation reactions (strongly and weakly bonded versions); and
- redox reactions, in particular including the oxidation of pyrite to control amounts of Fe(III) and sulphate when oxygen is available, and the conversion between sulphate and sulphide.

In [14] the processes were simulated using equilibrium assumptions, except for pyrite dissolution, which was treated kinetically. QPAC-EBS includes a chemistry module that is capable of representing a range of geochemical processes, including both kinetic and equilibrium reactions. For the preliminary modelling described in [3], the system outlined above was simplified and only the trace solids were simulated since the main aim was to compare bentonite erosion rates with those presented by SKB [13], which was assumed to be controlled by the ability of gypsum to buffer calcium ions in the porewater.

Dissolution of gypsum is a potential source of sulphate by the reaction

$$\mathrm{Gypsum} = \mathrm{Ca}^{2+} + \mathrm{SO}_4^{2-} + 2\mathrm{H}_2\mathrm{O}$$

In the QPAC-EBS simulations, gypsum dissolution was modelled using kinetic data from [16], rather than instantaneous equilibrium assumed by SKB. Suggestions on how montmorillonite dissolution could be treated kinetically were also given in [3].

The exclusion of the redox reactions assumes that the bentonite contains no soluble pyrite, which affects the sulphate concentrations in the porewater and pH. Since the quantity of pyrite in the bentonite is expected to be small this is not expected to be a significant omission.

In the QPAC-EBS calculations, canister corrosion was assumed to be driven by the transport of sulphide to the canister surface. Sulphide is represented in the system by the HS^-ion. It was assumed that all sulphide ions arriving at the canister surface are immediately consumed in the corrosion process, and thus a zero sulphide concentration was set on the boundary at the canister surface. The resulting sulphide flux at the surface can be converted into a corrosion rate ($m\ y^{-1}$) by means of a suitable conversion factor.

Since redox reactions in the porewater were omitted from the simplified system there is no mechanism to convert the sulphate that is generated from gypsum dissolution to sulphide. Hence the simplification also has the effect of reducing the potential amount of corrosion at the canister surface. However, this simplification should be viewed in the context of the other uncertainties that are present in the model. Furthermore, the omission of more detailed kinetically-controlled reactions throughout the system is likely to have a large effect on the porewater compositions that are calculated. With the simplification of no redox reactions, the sulphide species is inert until it comes into contact with the canister surface, where it can take part in the corrosion reaction.

Conceptual models of geometry and erosion

Chemical erosion of the bentonite occurs when the concentration of key divalent cations in the porewater becomes critically low, at which time the bentonite gel structure becomes unstable and the gel becomes a colloidal dispersion, referred to as a sol. This critical concentration, called the critical coagulation coefficient (CCC) is expressed in terms of the concentrations of the divalent calcium ion. In the QPAC-EBS model, as in [15], the CCC is assumed to be represented by the concentration of the Ca^{2+} ion and a value of 10^{-3} mol 1^{-1} is assumed, although SKB acknowledge that there is some uncertainty regarding the precise value. Model calculations are sensitive to the precise value that is chosen.

Both 2D and 3D geometries were considered, with the 3D system being modelled using cylindrical coordinates. A thin 2D cylindrical region representing the fracture (a thin annulus) intersects the 3D cylindrical region that represents the buffer. The innermost 15 cm of the fracture annulus is assumed to be filled with bentonite that has intruded into the fracture during swelling; this is the anticipated depth of intrusion obtained from modelling studies referred to by SKB [13]. This length of penetration of bentonite is fixed throughout the modelling by the same argument used in the 2D model. The model stretches 20 m radially from the central axis of the canister. At this distance it is assumed that the perturbation to the regional flow field introduced by the EBS is sufficiently small that the regional head drop can be applied consistently along the boundary.

The discretised 3D system is shown in Figure 24. In this figure the fracture is shown in blue and the bentonite in the buffer and fracture regions in red. Volumes show relative compartment sizes, hence the apparent distortion of the aperture as *r* increases.

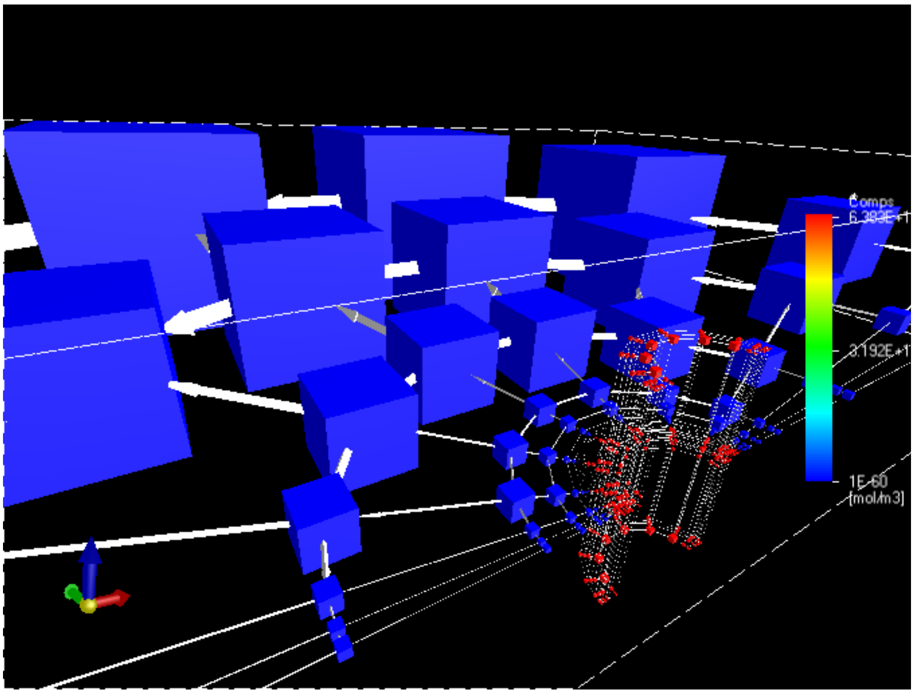

Figure 24
3D View of the modelled domain

A range of assumptions were made about the erosion process, designed to gain an understanding of the likely profile of Ca^{2+} concentration in the bentonite, since it is this that controls the potential destabilising of the bentonite, rather than the presence of gypsum, as was assumed in [13]. Three erosion models were considered (T1, T2 and T3):

- (T1) A no erosion case, in which bentonite is not assumed to erode even if gypsum is depleted or the Ca^{2+} concentration falls below the CCC. This is an optimistic case, since bentonite flow and transport properties are used throughout the bentonite regions in the domain.

- (T2) An erosion case (without continual gel intrusion) where erosion is assumed to occur as soon as the local gypsum inventory is exhausted (independent of whether the Ca^{2+} concentration falls below the CCC, and like the assumption made in the 2D modelling). Bentonite regions where the gypsum inventory is depleted effectively become ‘open water’ compartments as the bentonite is removed.

- (T3) As T2, but erosion is only assumed to occur once the Ca^{2+} concentration has fallen below the CCC. This is more consistent with the CCC model as described in [15] and allows gypsum neighbouring a location of local gypsum depletion to buffer the local Ca^{2+} concentration. Bentonite regions where this occurs effectively become ‘open water’ compartments as the bentonite is removed.

The permanent penetration distance of the bentonite into the fracture was not modelled in any of the simulations, since to model this process and conserve mass it would be necessary to include mechanical processes for solid mass transfer in the models; this could be considered in a future study. Making this assumption allows the bentonite in the buffer region to degrade through depletion of trace minerals ion some calculations. This acts to increase porosity in the buffer and enhance transport, thus increasing the amount of corrosion. Hence in this sense it is a conservative assumption.

In the first case, T1, not assuming immediate colloidal erosion of the bentonite allows the examination of the diffusive profile of the Ca^{2+} ions within the bentonite as gypsum is removed from the outermost section of the intruded bentonite. This allows investigation of whether the relatively large gypsum inventory in the buffer region is able to diffusively buffer the Ca^{2+} concentration length once gypsum is removed at the extremity of the bentonite penetration into the fracture. It is possible that sufficiently high Ca^{2+} concentrations will exist in the vicinity of the intact gypsum front that the colloidal instability may not occur instantaneously (as was assumed in [13]).

In the second case, T2, not assuming that fresh bentonite can continue to intrude into the fracture means that once the bentonite gel in the fracture is eroded, bentonite erosion can start to occur in the region of the deposition hole.

The third case, T3, is similar to T2, but allows the effect of ‘diffusive buffering’ of Ca^{2+} ions in the bentonite to be considered. Once gypsum has been depleted there is no local mineral buffering and so in T2 the bentonite is assumed to erode immediately. T3 allows the buffering capacity of gypsum in neighbouring locations to be represented, the effect of which will be limited by the rate at which Ca^{2+} ions can diffuse into the original location. This model is more consistent with the colloidal instability model for bentonite.

Porewaters

The chemical processes that need to be considered essentially occur over the entire evolution of the system, but erosion processes only pertain to the period of intrusion of glacial meltwaters, and thus occur later in the system evolution. In the current set of calculations only the period following the intrusion of glacial meltwaters was considered, in order to allow direct comparison of results with those from the physically-based models presented in

[13]. However it would also be possible to simulate the earlier evolution of the system in the QPAC-EBS model, with the onset of glacial meltwater interaction represented in the calculations by a change in boundary conditions. The natural host rock boundary water would change to very dilute meltwater, in which the Ca^{2+} concentration in particular is very low. QPAC-EBS allows changes in boundary conditions can be treated as either a continuous or discreet event.

In order to enable comparisons to be made with the physically-based calculations undertaken by SKB [13], whilst attempting to maintain a realistic (albeit simple) chemical model consistent with that presented by SKB in [14], the Grimsel ice-melt water composition from [13] was taken for the dilute water boundary condition and a modified version of the Laxemar porewater was taken as the initial condition porewater in the bentonite regions. The Ca^{2+} molality was modified to be consistent with the assumptions employed in [13], and the SO_4^{2-} molality was calculated assuming equilibrium with gypsum. All other porewater components initially in the bentonite were as specified in [14].

Illustrative calculations

In the T3 erosion model, the bentonite erosion process is implemented by monitoring the Ca^{2+} concentration and changing the state of the compartment (as represented by its flow and transport properties) from being bentonite to being open water when the concentration falls below the CCC.

The Ca^{2+} fluxes across the (initial location of) the gel/fracture interface are shown in Figure 25.

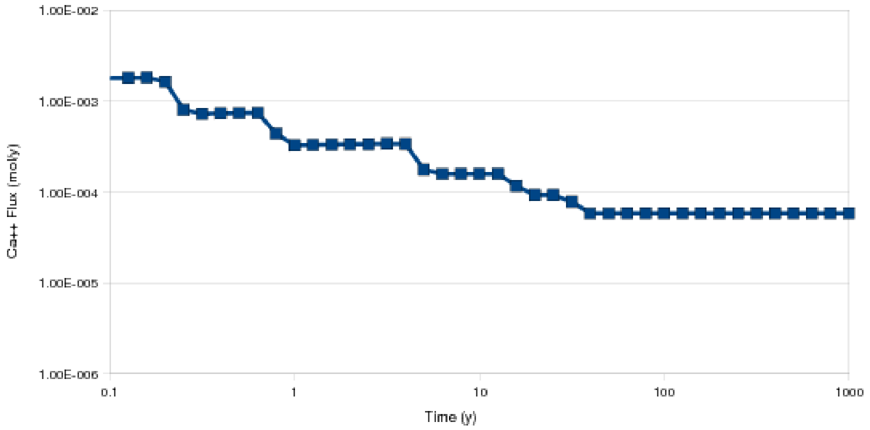

Figure 25
Net Ca^{2+} flux from the bentonite gel to the fracture

Figure 26 shows that by 50 years the gypsum in the fracture has all been lost and gypsum has dissolved completely to a distance of 5 cm inside the buffer (only in the plane of the fracture). This dissolution front then halts. The reason for the slowing of the front is that inside the buffer region there is a relatively large quantity of gypsum, which can diffusively buffer the Ca^{2+} concentration to prevent further dissolution of gypsum. This obviously cannot last indefinitely, but does last the 1000 y duration of the simulation.

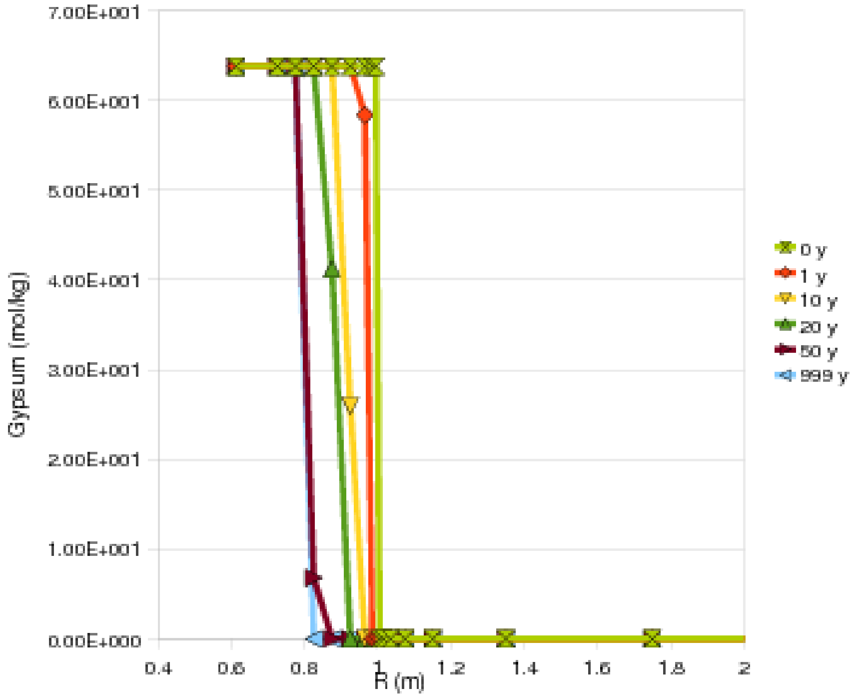

Figure 26
Gypsum profiles in the buffer (0.525-0.85 m) and fracture (0.85-1.00 m). The angle is 170-180^0 in the upstream direction.

The gypsum inventory can buffer the Ca^{2+} concentration is sufficient to maintain Ca^{2+} concentrations above the CCC up to around 7.5 cm into the bentonite gel in the fracture for over 1000 y, as shown in Figure 27. This would tend to suggest that if bentonite fluid motion is somehow inhibited at later times in the system, or if the maximum penetration distance of 15 cm is an over-estimate, then it is possible that erosion may not actually be possible, provided that the bentonite penetration distance remains below approximately 7 cm. The uncertainty in the precise value of the CCC is also an important factor, since if the true CCC is lower than the value assumed in the simulations then it is likely that diffusive buffering of the Ca^{2+} concentration will preserve more of the bentonite.

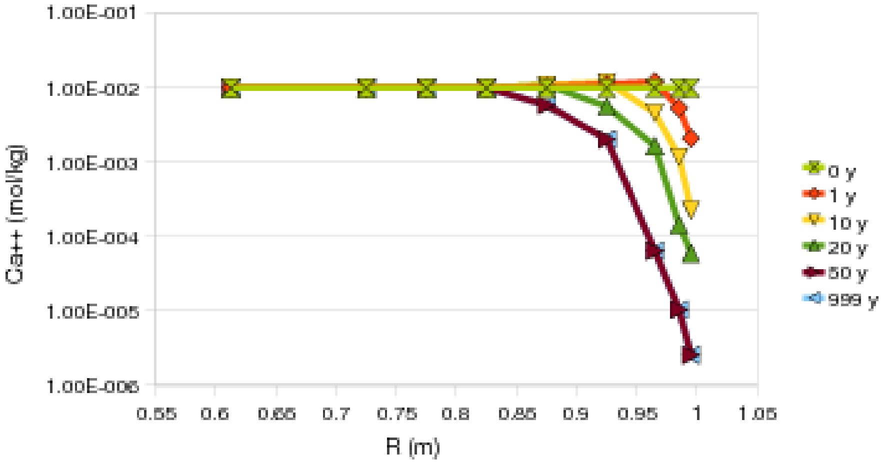

Figure 27
Ca^{2+} concentration profiles in the buffer (0.525 - 0.85 m) and the bentonite in the fracture (0.85-1.00 m). The angle is 170-180^0 from the upstream direction

Based on the 30 years that it takes for all of the gypsum in the bentonite gel to be dissolved, an erosion rate of around 5E-3 kg y^{-1} can be derived. The time taken for the Ca^{2+} concentration to fall below the CCC in the outermost 1 cm of bentonite gel, which is 5 years in this case, gives an erosion rate of 2.3E-3 kg y^{-1}.

The corrosion rate at the canister surface for the T3 model is shown in Figure 28 as a function of position along the canister height on the upstream and downstream faces of the canister. Results for the T1 model are almost identical with the calculated maximum rate of corrosion on the upstream face on the plane of the fracture being around 5E-13 m y^{-1}. SKB have published expected corrosion rates in the approximate range 1E-12 to 2E-10 m y^{-1} [8, Figure 9-62]. The value presented in this example calculation is therefore around half the SKB lower estimate.

Rates of corrosion around three orders of magnitude higher on the upstream face are seen in the T2 model (Figure 29). This model does not assume any ‘diffusive buffering’ due to Ca^{2+} diffusion and hence is more consistent with the SKB model [8], although it does not represent continual gel intrusion into the fracture, hence it represents a more pessimistic set of assumptions. The rate of corrosion on the upstream edge in this case is around twice the SKB upper estimate.

As previously indicated, these calculations are based on very preliminary modelling assumptions and parameter values.

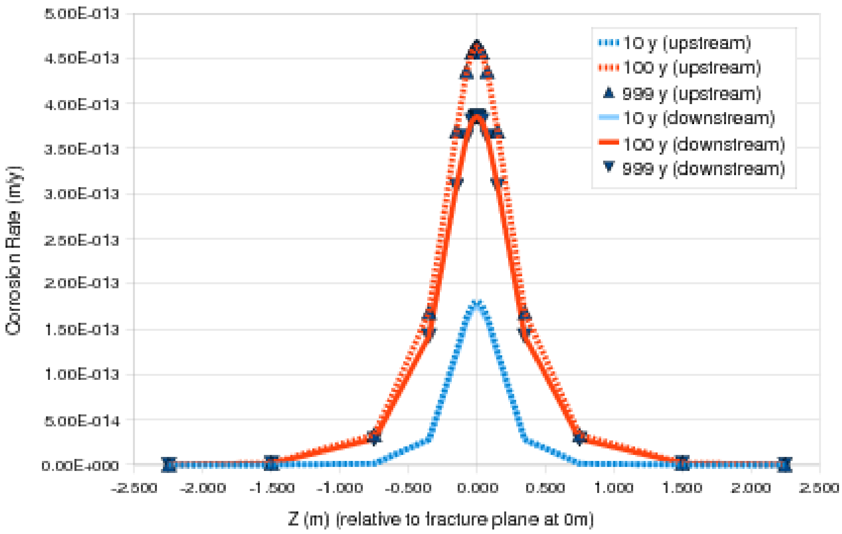

Figure 28
Corrosion rates along the canister length at 10, 100 and 1000 y in the T3 model. Results for the T1 model are almost identical.

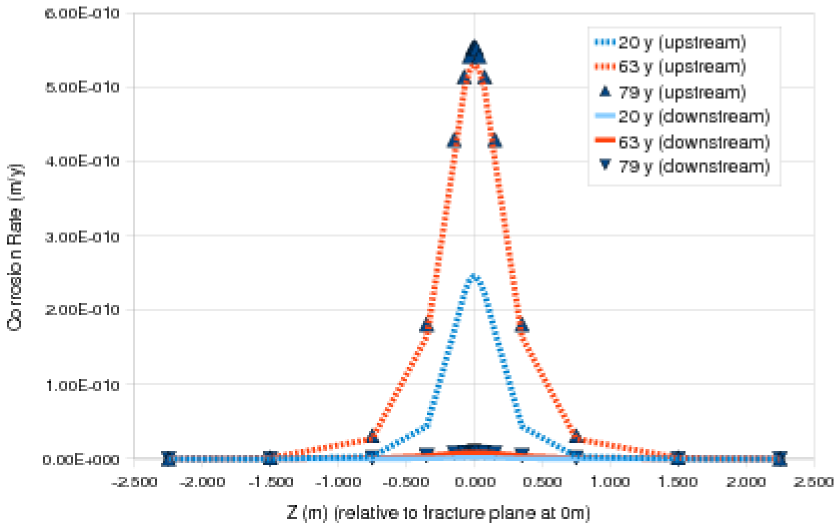

Figure 29
Corrosion rates along the canister length at 10, 100 and 1000 y in the T2 model. Upstream corrosion rates are much larger than downstream rates.

Discussion

The calculations presented in [3] represent early prototyping of the representation of the buffer erosion scenario using QPAC-EBS. They have helped to gain insight into the uncertainties related to bentonite erosion and the effect on corrosion, although only some of the relevant processes have been implemented. The key observation from the preliminary modelling undertaken so far is that basing the bentonite destabilisation directly on the Ca^{2+} concentration in the porewater rather than on the immediate presence of gypsum provides lower estimated rates of bentonite erosion. In future modelling consideration should be given to including the mechanical processes representing the penetration of bentonite into the fracture to derive more realistic loss rates.

The development of QPAC and the QPAC chemistry module was heavily influenced by Quintessa's earlier reactive transport code Raiden, which simulated fully coupled flow and geochemical reactions and was used extensively in the SKI programme over a number of years to model: pH buffering capacity of granite backfills at the particle scale [17] and vault scale [18]; solid-solution reactions for cement dissolution and coupling to evolution of physical properties in backfills [19]; and modelling degradation of low pH cements [20] and their interaction with bentonite [21].

The QPAC chemistry module incorporates the full range of processes that can be simulated with Raiden and so can be used to model the same type of systems, and additionally includes surface reactions and crystal growth/ripening processes as well as having access to the general time-dependent formulations that are possible in QPAC that have allowed it to model more complicated coupled systems, including: time-dependent clay sediment deposition, compaction and alkaline alteration at the Searles Lake natural analogue site [22] and iron-bentonite interactions [23].

8. Conclusions

The use of Quintessa’s general-purpose modelling code QPAC as the basis for software (referred to as QPAC-EBS) to investigate the evolution of engineered barrier systems in radioactive waste repositories has proved to be extremely successful. A satisfactory understanding of the evolution of the EBS is an essential part of the safety case for the repository, particularly as changes to the system in the period following repository closure could mean that the system will not perform as designed over long timescales.

It has been demonstrated that QPAC can provide the basis for sophisticated calculations involving coupled thermal, hydro, mechanical and chemical (THMC) processes using an approach that differs fundamentally from that taken by codes specifically designed to undertake such calculations. The ability to be able change modelling assumptions to investigate the importance of key processes provides a powerful regulatory review capability.

Studies undertaken to date have demonstrated that QPAC-EBS can be used effectively to investigate both the early evolution of the EBS when thermal effects and repository resaturation are important, and important scenarios for the later evolution of the system when buffer erosion and canister corrosion may occur. To date radionuclide transport calculations following canister failure have been undertaken with separate software, but it would be possible, if required, to couple consideration of EBS evolution to radionuclide transport using QPAC’s tracer transport module.

A key issue for modelling EBS evolution is the satisfactory modelling of the behaviour of the bentonite buffer. Bentonite is a difficult material to model, partly because of the complex coupled mechanical, hydro and chemical processes involved in swelling during resaturation. Models employed to date have generally taken an empirical approach, but a new model developed during the EU THERESA project could be further developed to provide a better representation of these processes during EBS evolution.

QPAC-EBS could play an important role in supporting SSM’s review of the forthcoming SR-Site assessment by SKB if used by Quintessa in independent supporting calculations.

9. References

[1] Quintessa. (2010) QPAC: Quintessa's General Purpose Modelling Software. Quintessa Report QRS-QPAC-11.

[2] Maul, P. R., Benbow, S. J., Bond, A. E. and Robinson, P. C. (2008). Independent Calculations for the SR Can Assessment. SKI Report 2008:12.

[3] Maul, P.R., Benbow, S.J., Bond, A.E., Robinson, P.C. and Savage, D. (2009) EBS Evolution Calculations using QPAC-EBS: A Progress Report for Work Undertaken in 2008. Quintessa Report QRS-3008C-1 version 1.1.

[4] Jacquet, O. and Siegel, P. (2004) Local-scale modelling of density-driven flow for the phases of repository operation and post-closure at Beberg. SKB Report R-04-46.

[5] Bond, A. and Watson, C.E. (2008) The Use of QPAC-EBS for Project THERESA Benchmarking Studies. Quintessa Report QRS-3009A-1 version 3.0.

[6] Bond, A.E., Maul, P.R., Savage, D. and Wilson, J. (2009). The Use of QPAC-EBS for Project THERESA Full-Scale Tests. Quintessa Report QRS-3009A-2 version 2.0.

[7] Bond, A.E., Maul, P.R., Robinson, P.C., Savage, D. and Wilson, J. (2009) The Use of the QPAC-EBS Code for Modelling the Evolution of Engineered Barrier Systems with a Bentonite Buffer. Paper given to the joint TIMODAZ/THERESA conference, Luxembourg September 2010.

[8] SKB (2006) Long-term safety for KBS-3 Repositories at Forsmark and Laxemar - a First Evaluation. SKB Report TR-06-09.

[9] Hedin (2004) Integrated Near-Field Evolution Model for a KBS-3 Repository. SKB Report R-04-36.

[10] Xie, M., Bauer, S., Kolditz, O., Nowak, T. and Shao, H. (2006) Numerical Simulation of Reactive Processes in an Experiment with Partially Saturated Bentonite. Journal of Contaminant Hydrology 83, 122-147.

[11] Bradbury, M. H. and Baeyens, B. (2002) Porewater Chemistry in Compacted Re-saturated MX-bentonite. Physicochemical Characterisation and Geochemical Modelling, PSI Report 02-10, Paul Scherrer Institute, Villigen, Switzerland.

[12] Sato, H. (2008) Thermodynamic Model on Swelling of Bentonite Buffer and Backfill Materials. Physics and Chemistry of the Earth

33(supplement 1), S38-S43.

[13] Liu, J. and Neretnieks, I. (2006) Physical and Chemical Stability of the Bentonite Buffer. SKB Report R-06-103.

[14] Arcos, D., Grandia, F. and Domenech, C. (2006) Geochemical Evolution of the Near Field of a KBS-3 repository. SKB Report TR-06-16.

[15] SKB (2004) Interim Process Report for the Safety Assessment SR-Can. SKB R-04-33.

[16] Palandri, J. L. and Kharaka, Y. K. (2004) A Compilation of Rate Parameters of Water-Mineral Interaction Kinetics for Application to Geochemical Modelling. Open File Report 2004-1068, United States Geological Survey, Menlo Park, California, USA

[17] Benbow, S., Robinson, P. and Savage, D. (2002) Buffering Capacity of pH in Backfill. SKI Report 02-39.

[18] Benbow, S., Watson, S., Savage, D. and Robinson, P. (2004) Vault-scale Modelling of pH Buffering Capacity in Crushed Granite Backfills. SKI report 04-17.

[19] Benbow, S., Watson, C. and Savage, D. (2005) Investigating Conceptual Models for Physical Property Couplings in Solid Solution Models of Cement. SKI Report 05-64.

[20] Benbow, S., Walker, C. and Savage, D. (2007) Intercomparison of Cement Solid-solution Models: Issues affecting the Geochemical Evolution of Repositories for Radioactive Waste. SKI report 07-29.

[21] Watson, C., Benbow, S. and Savage, D. (2007) Modelling the Interactio of Low pH Cements and Bentonite: Issues affecting the Geochemical Evolution of Repositories for Radioactive Waste. SKI report 07-30.

[22] Savage, D., Benbow, S., Watson, C., Takase, H., Ono, K., Oda, C. and Honda, A. (2010). Natural Systems Evidence for the Alteration of Clay under Alkaline Conditions: An Example from Searles Lake, California. Applied Clay Science 47, 72-81.

[23] Savage, D., Watson, C., Benbow, S. and Wilson, J. (2010). Modelling Iron-bentonite Interactions. Applied Clay Science 47, 91-98.

[24] Rutqvist, J., and Tsang, C.-F. (2008) Review of SKB's work on coupled THM processes within SR-Can: external review contribution in support of SKI's and SSI's review of SR-Can. SKI Report 2008:08.

Strålsäkerhetsmyndigheten
Swedish Radiation Safety Authority

SE-171 16 Stockholm
Solna strandväg 96

Tel: +46 8 799 40 00
Fax: +46 8 799 40 10

E-mail: registrator@ssm.se
Web: stralsakerhetsmyndigheten.se